

Effect of sputtering gas on structural and optical properties of nanocrystalline tungsten oxide films

Amit Kumar Chawla^a, Sonal Singhal^a, Hari Om Gupta^b, Ramesh Chandra^{a,*}

^a Nanoscience Laboratory, Institute Instrumentation Center, Indian Institute of Technology Roorkee, Roorkee — 247667, India

^b Department of Electrical Engineering, Indian Institute of Technology Roorkee, Roorkee — 247667, India

Available online 26 June 2008

Abstract

We report the effect of inert gas (argon and helium) along with different concentrations of oxygen on the structural and optical properties of the rf magnetron sputtered nanocrystalline tungsten oxide thin films. The crystal structure and surface morphology were studied by X-ray diffraction (XRD) and atomic force microscope (AFM), respectively. We find that the atomic mass of the sputtering gas significantly affects the primary crystallite size as well as the surface morphology and texture. We were able to relate the higher oxidation of the tungsten atoms with low partial pressure of oxygen when films are deposited in helium instead of argon. It was also observed that the bandgap of the WO₃ films increases with increase in the partial pressure of oxygen.

© 2008 Elsevier B.V. All rights reserved.

Keywords: Tungsten oxide; XRD; AFM; rf sputtering; Penning ionization

1. Introduction

Thin films of transition metal oxides have attracted a great deal of attention because of their important applications such as electrochromic devices and solid state sensors. Recently the electrochromic devices made by using the electrochromic oxides like tungsten oxide have been extensively studied to regulate the radiated energy through glass with modifying their optical properties for the application in ‘smart windows’ [1–6]. Physical properties (e.g., electrical conductivity) of WO₃ depend on surrounding gaseous atmosphere because of physisorption, chemisorption and catalytic reactions between gases and material surface. For this reason, thin films of such material were tested for gas sensing application [5].

WO₃ thin films have been prepared by various methods including vacuum evaporation [7], anodic oxidation [8], spray pyrolysis [9], sol–gel [10], pulsed laser ablation [4], molecular beam deposition [11] and sputtering [5]. The physical properties of a material are seriously affected by structural order and

morphology. Different preparation methods have respective advantages in film quality and production cost in viewpoint of material applications. A profound knowledge of the structure and stability of WO₃ thin films is of importance for their effective use in practical device applications. We have used rf magnetron sputtering for the synthesis of nanocrystalline tungsten oxide thin films by varying oxygen ratio with argon and helium. Similar studies for other sputter-deposited nanocrystalline films are quite rare. In this paper we have shown how the nature of the sputtering gas (argon and helium) along with oxygen concentration affects the surface morphology, texture and the optical properties of the nanocrystalline tungsten oxide films.

2. Experimental details

Tungsten oxide nanocrystalline thin films were deposited by rf magnetron sputtering in a custom designed 12"-diameter chamber (Excel Instruments). The chamber was initially evacuated to about 10⁻⁶ Torr by a turbomolecular pump backed by a rotary pump. Thereafter, a high purity (99.9%) inert gas (He and Ar) with different oxygen partial pressures ranging from 10 to 40% was bled into the chamber. The ratio of the gas mixtures was controlled and measured using mass flow

* Corresponding author. Tel.: +91 1332 285743; fax: +91 1332 286303.
E-mail address: ramesfic@iitr.emet.in (R. Chandra).

controller and capacitance manometers (MKS) respectively. The gas pressure was kept at 15 mTorr for all depositions. During each sputtering experiment, the gas pressure was carefully monitored and kept constant since the sputtering current is extremely sensitive to the pressure of the sputtering gas. Sputtering was done for a set period of time at a fixed power of 100 W and the substrates (glass plates) were kept at 400 °C. The substrates were kept 50 mm away from the 2" diameter tungsten target of 99.97% purity. Other than the sputtering gas, all parameters were kept constant during the set of experiments reported here.

The WO₃ films were characterized by XRD for the structural properties by using X-ray Diffractometer (Bruker D8 Advance). The coherently diffracting domain size (d_{XRD}) was calculated from the integral width of the diffraction lines using the well known Scherrer equation after background subtraction and correction for instrumental broadening. The surface morphology and the microstructure of the films were studied using Atomic Force Microscope (NT-MDT Ntegra). Optical reflectance and absorption were measured in the 200–800 nm wavelength range using UV–Vis–NIR spectrophotometer (Cary 5000 Varian). Samples A, B, C and D were deposited in Ar–O₂ mixture with oxygen partial pressure of 10, 20, 30 & 40% respectively while samples E, F, G and H were deposited in He–O₂ mixture with oxygen partial pressure of 10, 20, 30 and 40% respectively.

3. Results and discussion

Nanocrystalline WO₃ films were deposited using two different inert gases with different partial pressures of oxygen at same temperature and sputtering power. Fig. 1 shows the XRD pattern of the nanocrystalline thin films of WO₃ deposited in Ar–O₂ mixture with different oxygen partial pressures. Samples A, B, C and D were deposited in Ar–O₂ mixture with oxygen partial pressure of 10, 20, 30 and 40% respectively. It is evident from Fig. 1 that at low oxygen partial pressure the film (sample A) is a randomly oriented mixed phase (W and WO₃)

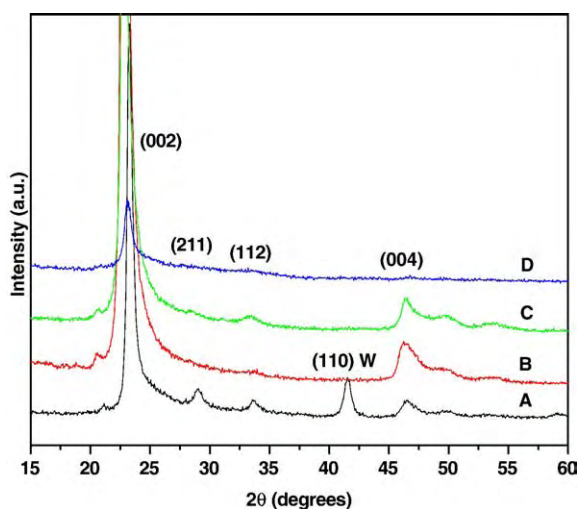


Fig. 1. XRD patterns of the WO₃ films in Ar–O₂ at different oxygen partial pressures.

while with an increase in oxygen partial pressure the film (samples B, C and D) becomes single phase (WO₃). This clearly indicates that the oxidation of the tungsten atoms is incomplete in oxygen partial pressure of 10% and it results in traces of tungsten metal atoms in the film (sample A).

Fig. 2 shows the XRD pattern of the nanocrystalline thin films of tungsten oxide deposited in He–O₂ mixture with different oxygen partial pressures. Samples E, F, G and H were deposited in He–O₂ mixture with oxygen partial pressure of 10, 20, 30 and 40% respectively. It is evident from Fig. 2 that at low oxygen partial pressure the film (sample E) is amorphous while with increase in oxygen partial pressure the samples become crystalline with (002) orientation.

It is observed that there is no tungsten peak in the sample deposited in He–10%O₂ atmosphere (Sample E). This means that oxidation of tungsten atoms can be achieved at low partial pressure of oxygen by replacing argon with helium. A potential reason for this is the process of penning ionization that occurs in plasma. In penning ionization process, some particles in the ground state, such as O₂ are ionized by transfer of the energy of rare gas atoms in neutral excited metastable states. Among the rare gases, helium in neutral excited metastable state (He*) has the highest energy i.e. helium can easily ionize O₂ since the energy of He* (19.82 eV) is higher than the first ionization potential of O₂ (12.06 eV) while Ar* cannot ionize O₂ through the penning ionization process because it has lower energy (11.55 eV) [12,13]. Thus during the preparation of the oxide films by reactive sputtering using helium gas, there is a possibility of enhancement of the reaction of metal atoms with oxygen because of an increase in activated particles of oxygen through the penning ionization process. We have calculated the thickness of the samples using the optical data. We have observed that by replacing the Ar–O₂ mixture with He–O₂ the thickness gets decreased by a factor of ~5. This decrease in deposition rate for a given partial pressure of oxygen would lead to an increase in the ratio of oxygen molecules and ions impinging on the surface per each W atom. Thus we can say that decrease in deposition rate by replacing the Ar–O₂ mixture with He–O₂ is also one of the potential reasons for the oxidation of tungsten atoms at low partial pressure of oxygen in helium along with penning ionization.

In order to calculate the particle size, d of the samples we have used the Scherrer formula [14]

$$d = \frac{0.9\lambda}{B \cos \theta_B}$$

where λ , θ_B and B are the X-ray wavelength (1.54056 Å), Bragg diffraction angle and line width at half maximum. The calculated particle sizes are shown in Table 1. It was observed that the films deposited in He–O₂ gas mixture have smaller particle size as compared to those deposited in Ar–O₂ gas mixtures. This can be explained on the basis of mean free path. The mean free path of the atoms in a gas is given by [15]:

$$\lambda = \frac{2.33 \times 10^{-20} T}{(P \delta_m^2)}$$

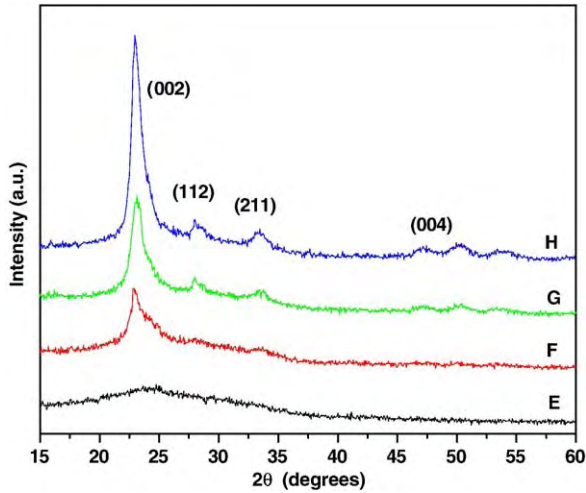


Fig. 2. XRD patterns of the WO_3 films in He-O_2 at different oxygen partial pressures.

where T is the temperature, P is the pressure and δ_m is the atomic (or molecular) diameter of the sputtering gas. Thus as the size of the sputtering gas atoms increases the mean free path of the inert gas atoms decreases and hence the collision frequency increases. We can therefore expect that as the diameter of the gas molecule increases the sputtered tungsten atoms would also undergo multiple collisions leading to a higher probability of agglomeration and growth even before arriving at the substrate. In such a case, we would expect an increase in the particle size with increase in atomic mass of the sputtering gas [16].

The AFM micrographs of the films deposited in argon and helium with 10% O_2 partial pressure are shown in Fig. 3. It is evident from the AFM figures that the particle size is large in case of sample deposited in argon as compared to that deposited in helium atmosphere and hence confirms the XRD result. However the overall particle size shown by AFM is much higher as compared with that calculated from the XRD line broadening. This is because of the fact that the XRD gives the average mean domain size while AFM shows agglomeration of the particles.

The transmittance spectra for the samples deposited in Ar and He atmospheres with different concentrations of O_2 are shown in Fig. 4a and b respectively. The oscillations in the

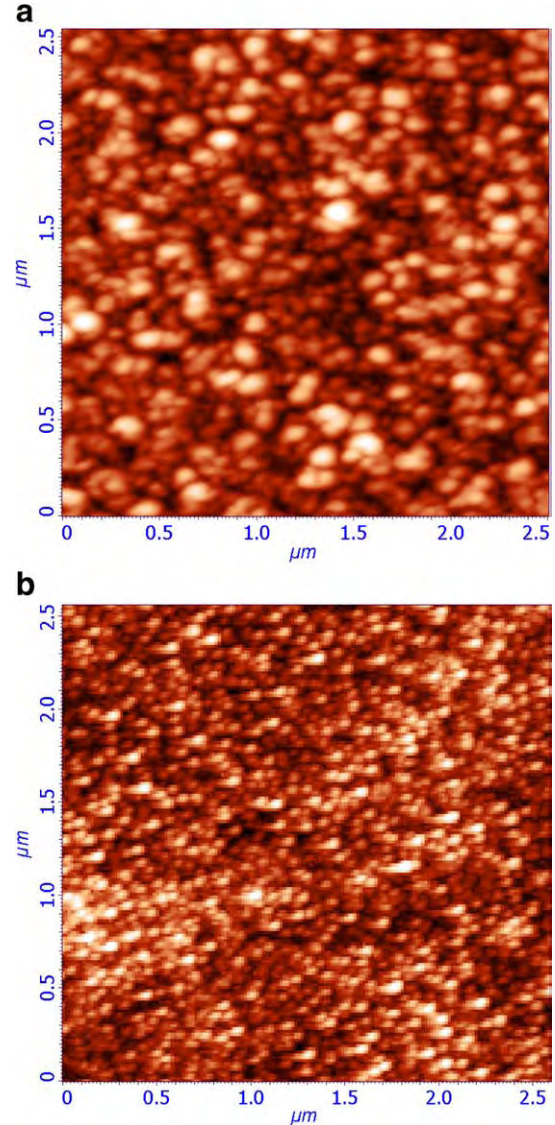


Fig. 3. AFM images of the WO_3 deposited in 10% O_2 in (a) argon (b) helium.

spectrum with wavelength are due to interference effect. It was observed that the transmittance of the WO_3 films increases with increase in the oxygen partial pressure. From literature it was evident that the optical transmittance of the WO_3 film depends on the oxygen content of the films [1]. Thus the increase in transparency of the films deposited at elevated oxygen pressure is attributed to the fall in the density of oxygen ion vacancies in the oxygen rich films. No effect of the inert gas used was seen on the transparency except the one deposited with 10% oxygen concentration in argon atmosphere.

The transparency of the sample deposited in argon atmosphere with 10% oxygen concentration [Fig. 4a] is almost zero in the visible region except 20% transparency in the wavelength range of 400–500 nm. Due to this the sample appears blue in color while all other are transparent [4]. The origin of this blue color is due to the presence of oxygen vacancies (i.e. WO_{3-y}) associated with tungsten ions in lower oxidation states than the 6+ expected in WO_3 stoichiometry.

Table 1
Calculated parameters of the tungsten oxide thin films

Sample name	Sputtering gas	d_{XRD} (nm)	Band gap (eV)	Refractive index	Thickness (nm)
A	Ar+10% O_2	15.2	2.76	–	–
B	Ar+20% O_2	14.5	2.87	2.91	902
C	Ar+30% O_2	14.9	2.93	2.93	1395
D	Ar+40% O_2	14.7	3.07	2.99	1298
E	He+10% O_2	–	2.98	2.85	197
F	He+20% O_2	9.3	3.04	2.97	297
G	He+30% O_2	9.7	3.13	2.99	257
H	He+40% O_2	9.5	3.22	2.98	342

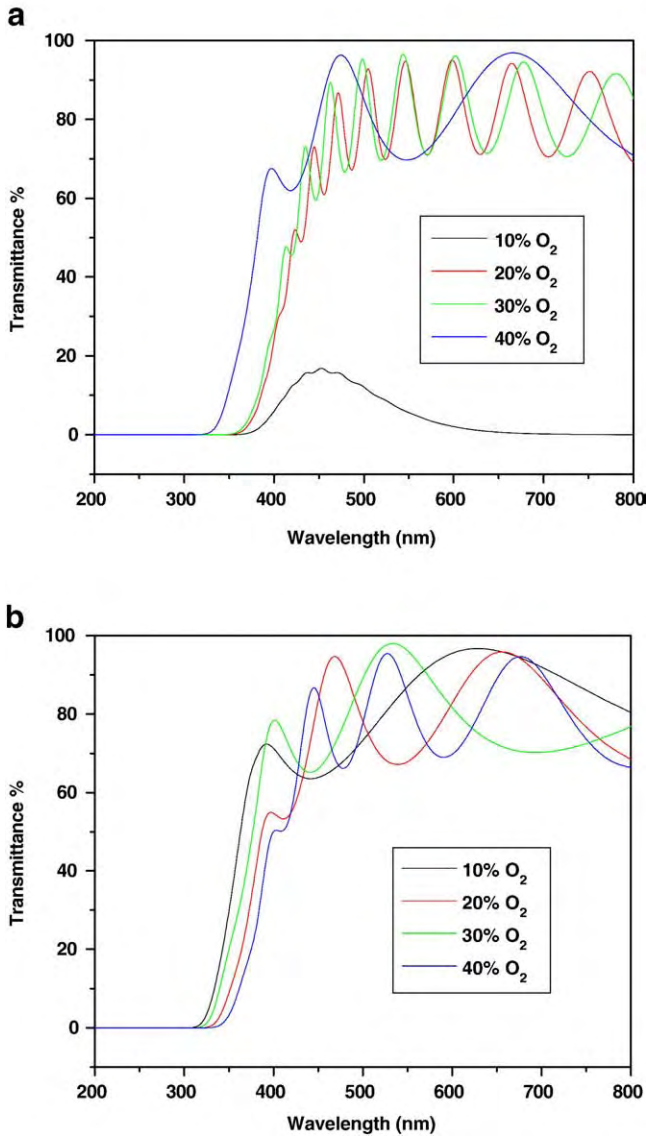


Fig. 4. a Optical transmission curve of WO₃ films deposited at 400 °C in Ar–O₂ at different oxygen partial pressures. b Optical transmission curve of WO₃ films deposited at 400 °C in He–O₂ at different oxygen partial pressures.

The transmission data is used to obtain the refractive index of the film by using a model proposed by Manifacier et. al. [17]. According to this model the refractive index can be given by the equation

$$n = \left[N + (N^2 - n_0^2 n_1^2)^{1/2} \right]^{1/2} \quad (1)$$

where

$$N = \frac{n_0^2 + n_1^2}{2} + 2n_0 n_1 \frac{T_{\max} - T_{\min}}{T_{\max} T_{\min}}$$

where n_0 and n_1 are the refractive indices of air and the substrate (glass here) respectively. Eq. (1) shows that the refractive index, n of the nanocrystalline WO₃ films can be

explicitly determined from T_{\max} , T_{\min} , n_0 and n_1 at the same wavelength. The refractive index calculated using these formulas is given in Table 1. We have also calculated the thickness of the deposited films using the relation

$$t = \frac{M \lambda_1 \lambda_2}{2[n(\lambda_1) \lambda_2 - n(\lambda_2) \lambda_1]}$$

where M is the number of the oscillations between the two extrema ($M=1$ between two consecutive maxima or minima). λ_1 , $n(\lambda_1)$ and λ_2 , $n(\lambda_2)$ are the corresponding wavelength and indices of refraction. We saw that the films deposited in Ar–O₂ mixture are 4–5 times thicker than the ones deposited in He–O₂ mixture. Generally the average grain size of films grown by sputtering increases as a function of film thickness. Thus an increase in the particle size is expected by replacing He–O₂ mixture with Ar–O₂ mixture. The same is observed in the results obtained from both XRD and AFM.

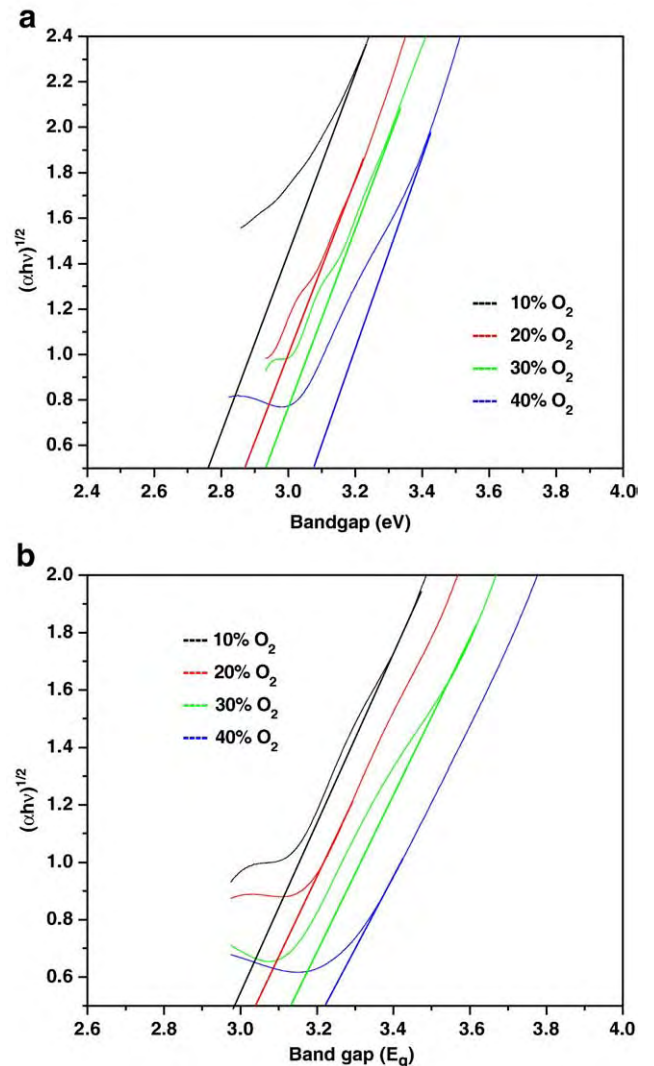


Fig. 5. a Optical absorption curve of WO₃ films deposited at 400 °C in Ar–O₂ at different oxygen partial pressures. b Optical absorption curve of WO₃ films deposited at 400 °C in He–O₂ at different oxygen partial pressures.

The absorption spectra of the nanocrystalline WO₃ was recorded as a function of the photon energy, $h\nu$, in the wavelength range 200–800 nm. The indirect optical bandgap (E_g) of nanocrystalline WO₃ was determined from the absorption coefficient (α) using the Tauc relation [18].

$$Y = \alpha h\nu = B(h\nu - E_g)^m$$

where $h\nu$ is the energy of the incident photons and E_g is the value of the optical band gap corresponding to transitions indicated by the value m which is 2 for indirect band gap semiconductor. The factor B depends on the transition probability and can be assumed to be constant within the optical frequency range. An extrapolation of the linear region of a plot of $(\alpha h\nu)^{1/2}$ on the y -axis versus photon energy ($h\nu$) on the x -axis gives the value of the optical bandgap E_g since $E_g = h\nu$ when $(\alpha h\nu)^{1/2} = 0$. Graphs between $(\alpha h\nu)^{1/2}$ and $h\nu$ for the samples deposited in different oxygen concentrations in argon and helium atmospheres are shown in Fig. 5a and b respectively. The bandgap values are shown in Table 1.

It is observed that the bandgap values of nanocrystalline films of WO₃ deposited in He+O₂ atmosphere are greater than that of in Ar+O₂ atmosphere. This can easily be explained on the basis of the XRD data and the AFM micrographs. Both XRD and AFM show that the particle size is bigger in argon than that of in helium and calculated bandgap values indicate the same. It is also observed that with increase in oxygen concentration the bandgap of the WO₃ films increases irrespective of the inert gas used. The reason for this may be attributed to the increase of oxygen concentration in the samples with increase in the oxygen percentage in the sputtering gas.

4. Conclusion

We have reported a systematic study of the optical and structural properties of the nanocrystalline tungsten oxide thin films deposited by rf magnetron sputtering in the presence of two different inert gases (argon and helium) with different concentrations of oxygen at same pressure, substrate temperature and sputtering power. XRD data indicates that the primary crystallite size in the nano-WO₃ films increases with increase in the thickness of the deposited samples (replacing helium by argon) and also with increase in the atomic mass of the sputtering

gas. The results on the tungsten oxide films show that oxidation of tungsten atoms can be achieved at low partial pressure of oxygen by replacing argon with helium. It is also interesting to remark that the bandgap of the films increases with increase in the oxygen partial pressure.

Acknowledgements

One of the authors, Amit Kumar Chawla, thanks CSIR, New Delhi for the award of senior research fellowship. The financial support by DST [Grant No. SR/S5/NM — 77/2002] and CSIR [Grant No. 03(1072)/06/EMR-II], New Delhi is gratefully acknowledged.

References

- [1] A. Subrahmanyam, A. Karuppasamy, Sol. Energ. Mat. Sol. C 91 (2007) 266.
- [2] G.A. de Wijs, R.A. de Groot, Phys. Rev. B 90 (1999) 16463.
- [3] A. Monteiro, M.F. Costa, B. Almeida, V. Teixeira, J. Gago, E. Roman, Vacuum 64 (2002) 287.
- [4] A. Rougier, F. Portemer, A. Que'de', M. El Marssi, Appl. Surf. Sci. 153 (1999) 1.
- [5] D. Manno, A. Serra, M. Di Giulio, G. Micocci, A. Tepore, Thin Solid Films 324 (1998) 44.
- [6] K. Miyake, H. Kaneko, M. Sano, N. Suedomi, J. Appl. Phys., 55 (1984) 2747.
- [7] W.H. Tao, C.H. Tsai, Sens. Actuators B 81 (2002) 237.
- [8] A. Dipaola, F. Diquarto, C. Sensuri, J. Electrochem. Soc. 125 (1978) 1344.
- [9] M. Regragui, V. Jousseume, M. Addou, A. Outzourhit, J.C. Bernede, B. El Idrissi, Thin Solid Films 397 (2001) 238.
- [10] M. Tong, G. Dai, D. Gao, Mater. Chem. Phys. 69 (2001) 176.
- [11] K. Iwata, P. Fons, S. Niki, A. Yamada, K. Matsubara, K. Nakahara, T. Tanabe, H. Takasu, J. Cryst. Growth 50 (2000) 214.
- [12] T. Fujii, T. Koyanagi, K. Morofuji, T. Kashima, K. Matsubara, Jpn. J. Appl. Phys. 33 (1994) 4482.
- [13] A.A. Kruihof, F.M. Penning, Physica 4 (1937) 430.
- [14] B.D. Cullity, Elements of X-ray Diffraction, 2nd edn., Addison-Wesley, London, 1978, p. 102.
- [15] L.I. Maissel, R. Glang, Handbook of Thin Film Technology, McGraw-Hill, New York, 1970, p. 1.
- [16] R. Chandra, A.K. Chawla, P. Ayyub, J. Nanosci. Nanotech. 6 (2006) 1119.
- [17] J.C. Manificier, J. Gasiot, J.P. Fillard, J. Phys. E: Sci. Instrum. 9 (1976) 1002.
- [18] J. Tauc (Ed.), Amorphous and Liquid Semiconductor, Plenum Press, New York, 1974, p. 159.